TECHNICAL ARTICLE



Aerospace, Energy Recovery, and Medical Applications: Shape Memory Alloy Case Studies for CASMART 3rd Student Design Challenge

Faith $Gantz^1$ • Hannah $Stroud^2$ • John C. Fuller³ • Kelsa $Adams^{4,5}$ • Peter E. $Caltagirone^6$ • Hande $Ozcan^2$ • Ibrahim Karaman² • Darren J. Hartl² • Aaron P. $Stebner^4$ • William $Trehern^2$ • $Travis\ Turner^7$ • Robert W. Wheeler¹ • Marcus L. $Young^1$ • Othmane Benafan⁶

Received: 24 February 2022/Revised: 8 April 2022/Accepted: 25 April 2022/Published online: 26 May 2022 © ASM International 2022

Abstract This collection of case studies presents a brief introduction of fundamental concepts for four SMA-based applications in the aerospace, energy, and medical fields designed by students and facilitated by professionals. The Consortium for the Advancement of Shape Memory Alloy Research and Technology (CASMART) Student Design Challenge is used as an outreach strategy to promote the implementation of state-of-the-art designs with SMA technology and is meant to inspire the next generation of SMA research. Student design challenge teams address real-world problems facing the SMA community and receive guidance and feedback from CASMART members. Student teams' hardware and materials deliverables had to meet basic function requirements specific to the application. Key results from seven teams (four hardware designs and three materials designs) highlight the design priorities,

processes, and challenges raised during development. The hardware designs used NiTi wires shape set and implemented by the students into prototypes for deployment and reorientation mechanisms in small satellites, linear generators to save energy, and a self-apply tourniquet design. Materials development explored the processability and material properties of CuAl-based and NiTi-based alloys for passive actuators in a deployment and reorientation mechanism for a small satellite, energy recovery from waste heat, and a pseudoelastic spinal curvature correction device.

Keywords CASMART · Shape memory alloy · Smart materials · Adaptive structures · Actuator design

Introduction

Since the 1960s, shape memory alloy (SMA) research and implementation has greatly contributed to transformative technologies in aerospace, biomedical, and automotive industries [1–11]. More recently, SMAs have been applied to solid-state refrigeration, passive seismic energy dissipation in structures, morphing aircraft wings, and pseudoelastic tires [12-16]. The thermomechanical and pseudoelastic properties of SMAs make powerful applications possible. The ability of SMAs to recover from large strains of 5 to 8% with little to no plastic deformation and to thermally actuate when under large stresses [17] makes them ideal for many varying applications. Their intrinsic multifunctional properties and high energy density enable the development of compact devices that can significantly reduce weight and size when compared with conventional systems. NiTi-based systems have produced energy density upwards of 10 MJ/m³, twice the value of hydraulics and

- Faith Gantz faithgantz@my.unt.edu
- Department of Materials Science and Engineering, University of North Texas, Denton, TX 76207, USA
- Department of Aerospace Engineering, Texas A&M University, College Station, TX 77843, USA
- ³ Additive Development, Relativity Space, Long Beach, CA 90815, USA
- Department of Mechanical Engineering and Materials Science and Engineering, Georgia Institute of Technology, Atlanta, GA 30332, USA
- Department of Mechanical Engineering, University of North Texas, Denton, TX 76207, USA
- Materials and Structures Division, NASA Glenn Research Center, Cleveland, OH 44135, USA
- Structural Acoustics Branch, NASA Langley Research Center, Hampton, VA 23666, USA



 $10 \times \text{to } 100 \times \text{more}$ than pneumatic and piezoceramic systems, respectively [2, 18]. Their advantages offer a paradigm shift in methods to generate renewable energy and geometric approaches.

Complexities stemming from the martensitic transformation and the coupled thermomechanical behavior pose significant challenges when integrating SMA systems into structural applications. Such complexities begin with fabrication methods due to material's sensitivity to compositional changes and the characteristics inevitable impurities. The iterative process of shape forming, shape setting, heat treating, and training changes the transformation temperatures, amount of recoverable strain, hysteretic width, among many other material properties. Each step influences microstructural features, thus effecting the thermal stability and fatigue life of SMAs [19-21]. The design process must address materials influence, in addition to system-level challenges, by adapting the composition and microstructure of the SMA to ensure the application's critical temperature and functional fatigue requirements are met. When integrating an SMA, the actuation strain and stress constraints are often considered to be analogous to displacement and force in conventional actuators. Directly employing unconventional actuators such as SMAs into conventional actuator applications will exhibit limitations to density and stroke length [22, 23]. These challenges motivated the creation of a collaborative space where discoveries could be made, information could be shared, resources could be combined to form standards for material preparation and testing, and to launch the field of SMAs forward.

In 2007, the Consortium for the Advancement of Shape Memory Alloy Research and Technology (CASMART) was formed to encourage collaboration and growth of SMA actuation technologies. Currently, CASMART consists of 26 member organizations, including partners in academia, industry, and government agencies, who work to promote the growth and adaptation of actuation technologies by achieving new understanding of the materials through experimentation and simulations to optimize designs and facilitate new applications. To achieve these goals and inspire the next generation of SMA researchers, CASMART hosts a biennial student design competition in which students can tackle real-world problems facing the SMA community while receiving guidance and feedback from CASMART members.

This manuscript is a compilation of designs from the third CASMART Student Design Challenge, held in 2019. It is meant to serve as a reference for SMA material creation and implementation by showcasing the work of

participating student teams and by documenting the difficulties they faced when designing SMA materials and systems. The CASMART Student Design Challenges have been used as an outreach strategy to promote the implementation of state-of-the-art designs with SMA actuators. The first competition, held in 2015, laid the foundations by establishing concepts fundamental to the process and parameters for designing structural and mechanical systems [24]. The second competition, held in 2017, built on the previous experience by introducing the concept of designing the material and designing with the material. The 2017 competition included seven teams from three different universities [25]. By 2019, student involvement had more than doubled, with a total of 14 teams and 49 individuals participating in the third design challenge. The premise of each design challenge was driven by real-world needs expressed by companies in the respective industries. The case studies were constructed to include two design perspective options: to design with the material or to design the material. Student teams' hardware and material deliverables had to meet basic function requirements specific to the application.

As a prelude to more detailed discussion of four design challenge case studies, this paper presents a brief introduction to the underlying concepts pertaining to these SMA-based applications, beginning with an overview of SMA technology. Four case studies are included:

- 1. Deployment and orientation mechanism for solar panels on SmallSats
- 2. Energy recovery from waste heat
- Tourniquet
- 4. Spinal curvature correction device

The Hardware Designs and Material Designs sections are divided into subsections for each respective application, providing objectives, constraints, and student teams' key findings. Commercially available SMAs were provided by manufacture/supplier sponsors to the hardware teams and fabrication methods and raw materials were made available to the materials teams upon request. Results are presented from seven of the 14 participating teams (four hardware designs and three materials designs) and highlight the design priorities, processes, and challenges raised during development.

Shape Memory Alloy Background

SMAs are unique for their ability to respond to change in structure and properties as a response to external stimuli. "Shape memory" refers to the ability of a material to return to a set shape, initiated by a phase transformation that is activated by elevating the material's temperature. This shape memory is the result of a solid-state phase change



¹ For more information about CASMART, please visit www. CASMART.org.

from martensite to austenite. As an SMA is heated, it transforms from martensite to austenite through a reversible, diffusion-less, solid-solid phase transformation. This capability produces three useful phenomena unique to SMAs: the shape memory effect, pseudoelasticity, and solid-state actuation.

The pseudoelastic effect describes the behavior of austenitic SMA under a load at a constant temperature above austenite finish temperature (A_f), a condition that induces a phase change from austenite to detwinned martensite, as shown in Fig. 1a). A complete phase reversal and strain recovery will occur upon unloading, thus resembling elasticity [26, 27]. A load may be applied to twinned martensite at a temperature below austenite start temperature (A_s) to create detwinned martensite. Upon release, the structure will remain detwinned and large strains can be observed (up to 10%). Heating the material above A_f will result in a transformation to the austenite phase and complete strain recovery, whereas cooling the material below martensite finish temperature (M_f) completes the cycle by returning to twinned martensite.

The solid-state actuation effect is when the material undergoes stress-induced phase transformation and then is thermally stimulated to produce actuation energy density (i.e., work output per unit volume). Thermal cycle, i.e., load-bias, tests are performed to determine the straintemperature characteristics as shown in Fig. 1b. The resulting characteristics are used for actuation specific properties such as transformation strain, work output, residual strain, and hysteresis. An applied load deforms the variants just enough to reorient and align them; however, the magnitude is much lower than the yield stress. The critical magnitude of stress is referred to as stress start (σ_s) and stress finish (σ_f) to complete the detwinning process. The reorientation is initiated at σ_s and requires the maximum σ_f to ensure all variants have adjusted to accommodate the load [28]. When additional stress is applied, dislocations (misalignments of atoms) form, increasing work hardening consequently to localized strain. The introduction of dislocations promotes a shift in transformation temperatures, providing an opportunity for thermal attunement. The tradeoff is the volume of the residual phase and stress increases. Work output is a product of the force applied and the change in strain between $A_{\rm f}$ and $A_{\rm s}$.

SMA Applications

Deployment and Orientation Mechanism for Solar Panels on SmallSats

Hardware Study I and II; Materials Study I One promising application for SMAs within the aerospace industry is utilization of the shape memory effect and solid-state actuation phenomena to create efficient actuation devices for small satellites, aptly termed "SmallSats." Two ways SMA actuators could be implemented in SmallSats are (1) as an active system (feedback controlled) in the deployment mechanism to deploy the solar panels and (2) as a passive system in the orientation mechanism to position the panels for maximum power collection [24]. Thus, the objective for this challenge was to design and build a deployment and orientation mechanism(s) with the use of SMAs that conforms to a 3U CubeSat weight and footprint.

A 3U CubeSat has dimensions of $10 \times 10 \times 30$ cm³ [29] at a cost which is two to three orders of magnitude cheaper than a full-scale platform, when including integration with the launch vehicle, launch, and ground operations [30]. CubeSats advantages of low cost, high functional density, short development cycle, and fast orbit entry, and allowing SmallSats to be widely used in research and education at universities [31]. The development of the CubeSat specification has provided a cost-effective platform on which to perform a variety of functions, including biological experiments in microgravity, communications network improvement, and advanced missions using constellations of many CubeSats working in conjunction [32]. Small satellite usage is not limited to government-sponsored research, however, and in recent years industrial

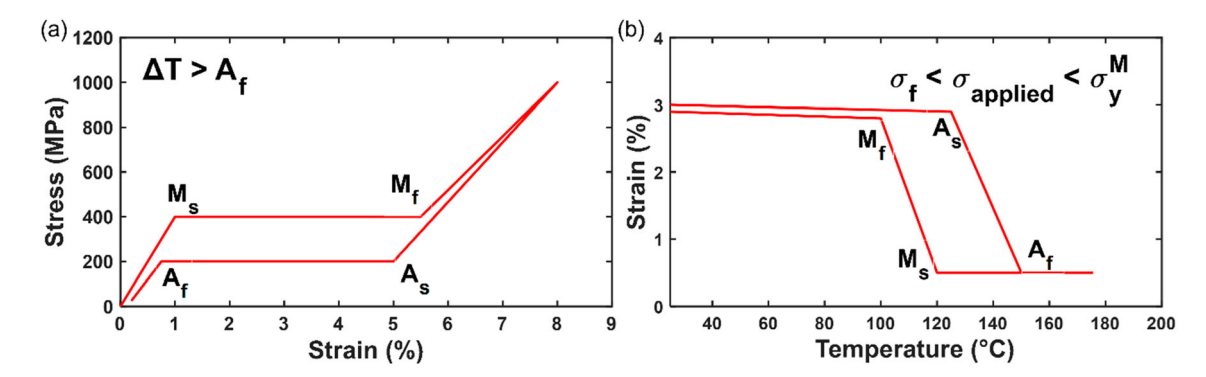


Fig. 1 Schematic of a hysteresis under the a pseudoelastic effect and b solid-state actuation



applications have created the need for government agencies, industrial leaders, and higher education establishments to work in tandem to achieve more complex goals. CubeSat designs help make that possible by allowing for standard commercial products within specific design and testing standards [29].

The challenge with utilizing these satellites is optimizing energy efficiency while minimizing cost. Therefore, the goal of this project was to improve the reorientation function of a microsatellite solar array to maximize absorption efficiency while using minimum power without adding additional weight. By using SMAs as a fully passive actuation system in the panels, the overall weight of the CubeSat can be reduced, and new systems could use one lightweight component to perform the actuation task when exposed to solar radiation. In view of the expense of every ounce of material sent into space, this reduction of weight could significantly reduce the cost of the satellite while maintaining the operational capabilities [30]. In terms of energy, the passive SMA actuator could replace actuators that must be powered internally rather than externally, thus reducing the mechanism's impact on the total energy budget of the craft. This development could result in an optimized power system in experimental spacecraft, opening the door to further research in weather patterns, communication capability, space exploration, and more [30]. Lower launching costs may create opportunities for smaller groups and private companies to begin novel research projects and bring lower cost products (such as communication devices) to market.

Energy Recovery from Waste Heat

Hardware Study III; Materials Study II Materials with high work energy density open the possibility of utilizing wasted heat by transforming it into other usable forms of energy. SMAs offer a unique solution when considering how the materials respond in a hot media flow between a hot and cold reservoir. These properties allow flexibility in the design and geometry of a waste heat recovery system, where thermal energy is converted directly to work output. The objective for this challenge was to design a cost-effective actuator system using an SMA material to capture thermal energy as the fluid media. The SMA would be affixed with an apparatus allowing the transfer of significant forces to mechanical power by utilizing wasted thermal energy.

A device designed to convert waste heat to useful power requires a combination of fluidic, mechanical, and electrical engineering designs and implementations. The fluids cycle through the hot reservoir as quickly as possible, with little fluid and thermal waste. The application of hot and cold fluids streams to the NiTi elements maximizes the

energy conversion efficiency. When the material responds by twisting or contracting, mechanical engineering is needed to convert the oscillatory motion into a rotary motion for an alternator, which is how the waste heat energy is converted to electrical energy. Utilizing waste heat sources is useful in engine exhaust and ambient air, thermal reservoirs, industrial heat exchangers, and geothermal applications. Each of these applications can be broken down to two scenarios: energy-harvesting gas or energy-harvesting water. There are three major challenges when designing a waste heat device: (1) implementing an SMA element while optimizing heat transfer between media (gas or water), (2) although a gas system is usually simple and inexpensive, exhaust gases have poor thermal transfer, and (3) wastewater transfers heat faster, but the designs are more complex.

Based on literature, forms that have been investigated with potential use in energy recovery devices are opencelled metallic foams, tubes, plates [33], or wire assemblies [34, 35]. Wire assemblies made with SMAs can be a beneficial approached to the heat exchange design by allowing a mixture of wires with different transformation temperatures, increasing the Carnot efficiency. The material response is affected by a combination of heat transfer coefficients, surface-area-to-volume ratio, and flow rates to optimize heat transfer. To date, low cycle time has been a limiting factor in SMA devices because of the longer timescale associated with convective heating kinetics as compared with the preferred method of joule heating [36]. Convective heat transfer is the primary method considered in this work, as directed by requirements from CASMART [37]. With either form of heat transfer media, the cost must be proportional to the application for the sake of the consumer. Hot exhaust systems for automotive applications tend to be simple and inexpensive, whereas consumers needing remote power systems will invest more for available power.

Tourniquet

Hardware Study IV The goal of this element of the design challenge was to develop a tourniquet system utilizing SMAs to supply compressive forces for stopping arterial bleeding in an emergency trauma situation. Mechanical designs focused on improving single-handed operation as compared with other state-of-the-art devices and on applying the correct compressive forces. To be competitive and accessible for emergency situations, the devices had to be compact, lightweight, rugged, and durable.

Tourniquets are life-saving devices used in surgical or field environments to provide time to treat life-threatening traumas, especially when the patient is in transport. Individuals often struggle to self-apply this medical device due



to trauma and operational difficulties. Exsanguination is the leading cause of death in active military zones and disaster areas, so the tourniquet needs to be reliable and function with simplicity. Traditional designs are painful to apply and challenging to operate single-handedly; another person is often needed to successfully apply the device to the patient. Simplifying the tourniquet-tightening mechanism could improve the speed of deployment and improve the success rate of self-application. Typical tourniquet-tightening mechanisms include windlass, ratchet, and bladder designs, but these are complex, bulky, and heavy. Many situations where a tourniquet would be needed, including the combat theater, require a compact design for lightweight travel. SMA devices provide a relatively lightweight method of actuation that could be used to occlude blood flow and simplify the process of tourniquet application.

Student teams were tasked with developing either a suitable material for use in an SMA tourniquet or a functional design for this application. The material's transformation temperatures had to be sufficiently low to prevent burn injuries to the user, and the device design was required to utilize the properties of SMAs to occlude blood flow in a designated limb. All the teams chose to focus on occluding the brachial artery in the arm. It was critical that the device be adaptable for various limb sizes and capable of being deployed using a single arm.

Spinal Curvature Correction Device

Materials Study III The goal of this challenge was to use an SMA in the design of an externally worn pseudoelastic brace that is more effective and comfortable than conventionally worn devices and offers an alternative to invasive spinal correction surgery [38, 39]. The SMA brace would provide effective therapy and maintain tension over time as compared with polymer-based designs.

Spinal orthoses (braces) can be designed based on the construction, rigidity, symmetry, openings, and principle of correction [40]. Rigid braces are considered more effective for curve correction than soft braces [41, 42]; however, both types have advantages and shortcomings. Rigid braces have a static nature, limiting motion and breathing, and weakening the muscles around the spine causing muscle atrophy. Materials commonly used to fabricate rigid braces are polyethylene, polycarbonate, and stainless steel to support and stabilize the patient's spine [38, 39]. Soft braces are typically made of textile fabrics and elastic bands to improve comfort and overall quality of life for the user [39]. The stiffness of the bands can be adjusted based on the severity of the needed treatment, allowing more relaxed bands to be used for preventing curve progression or for stabilization after surgery. Although the lower rigidity may prolong treatment time, soft braces promote muscle activity by strengthening the muscles around the spine [43].

The benefit of SMAs in this application is material longevity, as elastic wears out quickly and would require the brace to be refitted often. The pseudoelastic effect, activated by a patient's body temperature, can be used in orthopedic treatment to provide continuous and controllable corrective forces [39, 44]. Utilizing SMAs is an attractive option to produce a flexible device while maintaining the corrective benefits of a rigid brace. It is important, however, that the wires are not exposed to cooler temperatures, as this will deactivate the pseudoelasticity effect.

Hardware Designs

Deployment and Orientation Mechanism for Solar Panels on SmallSats

The objective for this challenge was to design a deployment and orientation mechanism for one or more solar panels with the use of SMAs.

The SmallSat hardware was required to comply with 3U CubeSat specifications in size, weight, and rigidity, Table 1. When stowed, the CubeSat was required to be $100.0 \pm 0.1 \text{ mm}^2 \text{ wide} \times 340.5 \pm 0.3 \text{ mm}$ tall. Foldable panels were allowed, but all designs were required to be deployed on demand and to stow back to initial position. The usable footprint (payload) could not exceed 0.5U and was required to be less than 20% of the gross 3U CubeSat weight. Rigidity refers to maintaining the designed shape while handling the launch loads [45], thermal environment, pressure changes, and gravitational loading. When operating, the orientation mechanism was to operate fully passive, with actuation time within 30 s and power level not exceeding 40 W. The deployment angle was to be equal to or greater than 90° from the stowed position. Lastly, no pyrotechnics were allowed, and no debris could be formed at any point in the mission. The reference NASA-STD-5017A was suggested as a guide to design the mechanism [46].

Hardware Study I

Team Sat³UNT: Kelsa Adams, Michael Ayers, Jordan Barnes, Robert Boone, David Evers, and Brittany Thurstin Team Sat³UNT from the University of North Texas determined the three mechanisms that would be employed in the design: retention, orientation, and deployment mechanisms. The retention and orientation mechanisms rely on steady-state actuation driven by thermally activated



Table 1 3U CubeSat hardware design requirements presented by CASMART challenge guidelines

Hardware requirement	Description	Functional requirement	Description
Dimensions (when stowed)	$100.0 \pm 0.1 \text{ mm}^2 \times 340.5 \pm 0.3 \text{ mm}$	Cycles	20 cycles/mission
Mechanism space/weight	Not to exceed $0.5U$, $< 100 g$	Actuation time	30 s
Rigidity	Conform to GSFC-STD-7000A	Power	< 40 W
		Deployment angle	> 90°

NiTi springs, and the deployment mechanism utilizes pseudoelastic springs to dampen the release of the panels to minimize residual accelerations. The retention mechanism uses a biasing spring to maintain the stowed position of the solar panels. Once the CubeSat reaches the desired altitude, the power supply sends a small amount of current to provide resistive heating to the SMA actuator, which allows the solar panels to move toward their active positions. The orientation mechanism incorporates two opposing SMAs to assist the solar panels in tracking the sun for maximum efficiency. The two opposing SMAs are connected to a single axis, which controls the rotation of the main solar panel. Like the first steady-state actuation application, the orientation mechanism is controlled by resistive heating. The deployment mechanism uses pseudoelastic springs to dampen deployment of the solar panels once they are released from the retention mechanism. Figure 2 shows (a) the SolidWorks displacement results for the highly damped model, (b-c) the retention mechanism, (d) the orientation mechanism, (e) the deployment mechanism, and (f) the final prototype design.

The CASMART spring design tool was used to determine the appropriate spring geometries capable of lifting the panels based on the projected mass. Fort Wayne Metals provided NiTi #6 wires, and students chose diameters of 1.0 and 0.25 mm for shape setting. The springs were shape set using a custom aluminum jig at 500 °C for 10 min. The retention mechanism was made from 6061 aluminum bar stock and measured $86 \times 86 \text{ mm}^2$ with a weight of 55 g. It used a single solid-state SMA extension spring requiring less than 10 W in 10 s under a load of 4 N and 5 mm stroke. Stainless steel bias springs, made by Classic Steel

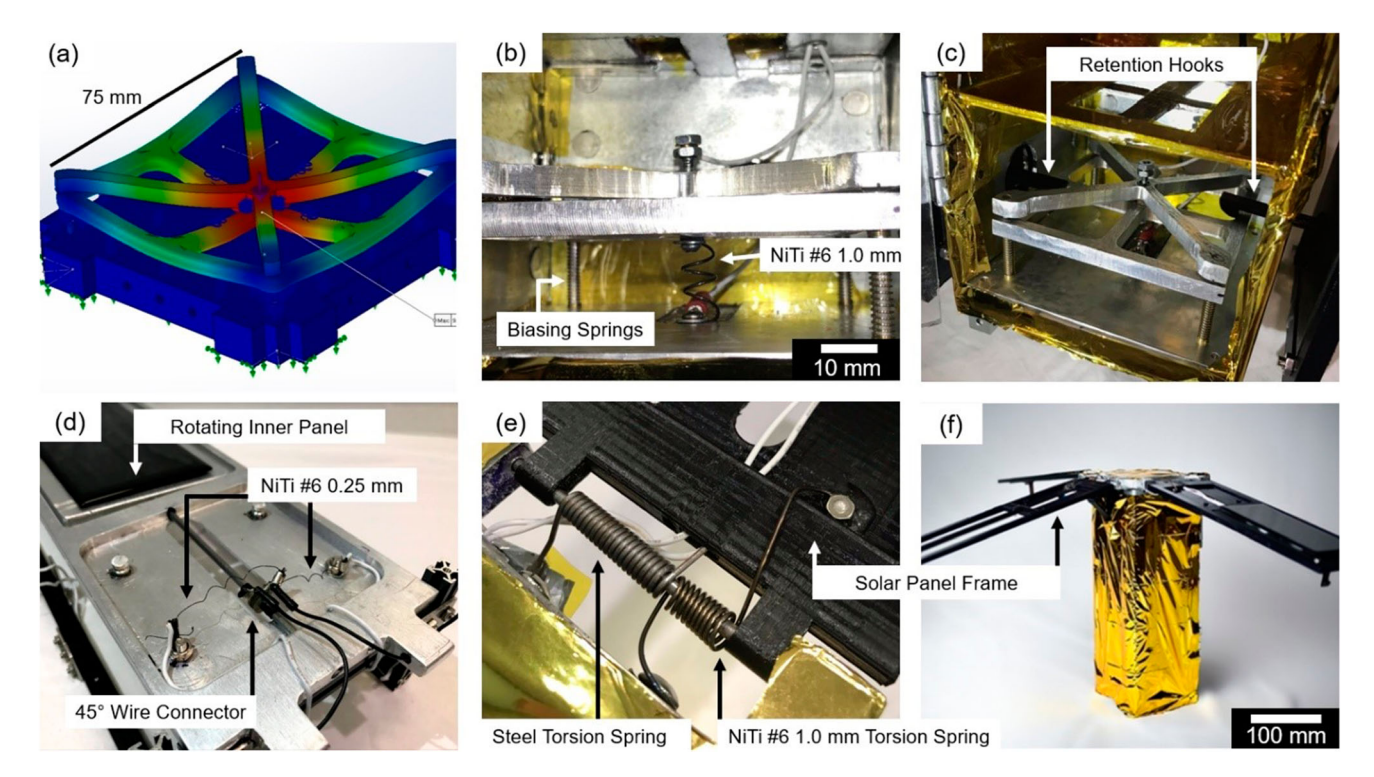


Fig. 2 A constructed prototype CubeSat utilizing nickel-titanium based shape memory alloy torsion and extension springs to articulate solar panels. a SolidWorks displacement results for the highly

damped model, **b**, **c** retention mechanism, **d** orientation mechanism, **e** deployment mechanism, and **f** final CubeSat



LLC, were used in the frame of the retention mechanism to provide return forces upon cooling of the NiTi wires. The orientation mechanism was set with the 0.25 mm diameter wire with three active coils of 3.2 mm diameter. One actuation stroke required less than 1 W under 5 s to achieve 45 rotations based on the CASMART spring design tool parameters of 1 N and 12 mm displacement. The final design used a torsional steel spring opposed by an SMA torsional spring.

Challenges were encountered in the manufacturing phase of the design process, as integrating the SMA components results in design complexity that can be remedied either through incorporation of more parts or through more intricate geometries. For this reason, polymer-based polylactic acid (PLA) additive manufacturing was used to construct the panel components. To summarize several of the key results and takeaways from this work:

- Determined optimal activation temperature range from 40 to 80 °C for the prototype demonstration using resistive heating with NiTi #6 wire shape set at 500 °C for 10 min.
- Designed and fabricated custom housings for the NiTi deployment, orientation, and retention mechanisms utilizing additive manufacturing for complex geometries.
- Implemented a passive-NiTi-driven orientation mechanism improving the CubeSat power collection efficiency by nearly 25% through use of (corresponding to ~ 1 W power gain) as compared with having no orientation mechanism.

Hardware Study II

Team PaST-Array: Will Machemer, Benjamin Pemble, Carlita Gorham, Forrest Denham, and Bryce Raymond Team PaST-Array from the Colorado School of Mines designed and tested a working prototype CubeSat capable of deploying solar panels and passive solar tracking enabling maximum collecting efficiency. The system accomplished this using a novel system of thermally activated NiTi springs oriented in a specific way to allow activation from solar radiation, which rotates the system, resulting in a panel orientation normal to the sun. The entire assembled system is shown in Fig. 3a. Three separate subsystems were designed to accomplish the deployment, upper rotation, and separate panel rotation: (1) latch mechanism, (2) rotation mechanism, and (3) wing actuation mechanism.

The latch mechanism was 3D printed using Onyx, a nylon mixed with chopped carbon fiber, although for the final design a high-grade machined aluminum may be more desirable. The latch mechanism can be released simply by

rotating the inner housing, as shown in Fig. 3b. An SMA spring affixed to the inner housing, along with a bias spring, will allow rotation upon thermal activation of the SMA spring, which will release the latch. When cooled, the locking mechanism returns to its original position with assistance from the bias spring. To relatch the system, the pin must simply be pushed into the latch slot (with assistance from the wing actuation mechanism), which will induce rotation and lock the housing around the latch.

The rotation mechanism (Fig. 3c) is also 3D printed using Onyx. The rotation mechanism takes up 0.5U of space and operates using 4 SMA springs and one bias spring. The design of the rotation mechanism allows for the sun to hit specific springs, while shading the others. When one of the springs is exposed to the sun, it will heat up from the solar radiation and induce rotation of the head. Using Fig. 3c as an example, when the sun hits SMA spring 1, it will actuate, causing a counterclockwise rotation. When the spring is no longer exposed to the sun, the bias spring assists in returning the mechanism to its original location. If multiple springs are exposed to the sun when only one spring should be exposed for proper actuation, polarized glass panels may be used next to the springs to allow solar radiation at only the desired angles (shown in light blue in the Fig. 3c.

The final mechanism for this system is the wing actuation mechanism, shown in Fig. 3d. This system is also designed to passively track the sun through the heating of SMA springs from solar radiation. The wing actuation mechanism uses two SMA actuation springs and two steel bias springs. Solar shades are built into the design so only one of the SMA springs at a time is exposed to solar radiation. When exposed, the SMA spring actuates, and the panel either lifts or lowers over the course of about 50 s. When the SMA spring is no longer exposed, the steel bias springs return the panel to a neutral position.

The latch, rotation, and actuation mechanisms were used to construct a successful prototype that was presented during the 2019 CASMART Student Design Challenge. To summarize a few key results from the work:

- Stock 1 mm diameter NiTi wire was shape set at 550 °C and used in the latch and hinge mechanism, and 0.038 mm NiTi wire was used for the head rotation mechanism. The design provided 3 degrees of freedom for solar panel articulation driven entirely by the 1 mm wire NiTi torsion springs.
- Onyx, a nylon, and carbon fiber material, was 3D printed to construct the complex geometries of the rotating head, hinges, and latch mechanism.
- The prototype was successfully tested with joule heating, but using convective heating (e.g., a heat



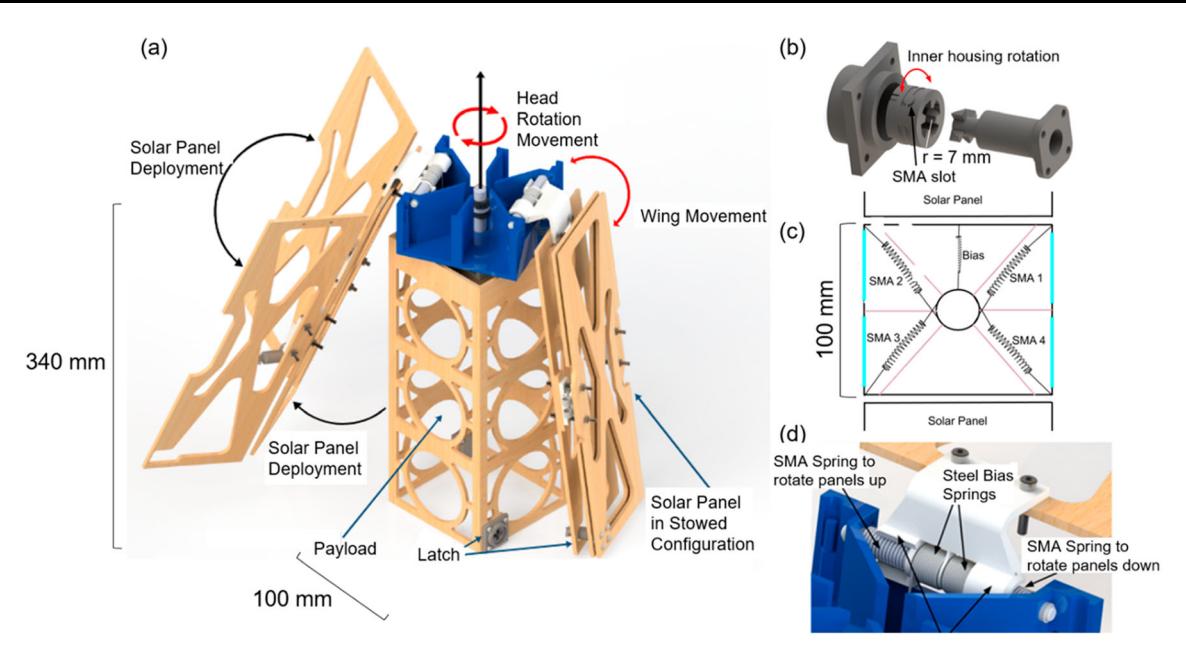


Fig. 3 a CAD render of the prototype design for a CubeSat structure with articulating solar panel shades and a rotating 'head' driven by thermally activated NiTi torsion spring and latching mechanism,

 ${\bf b}$ latching mechanism, ${\bf c}$ rotation mechanism schematic, and ${\bf d}$ wing actuation mechanism

gun) resulted in melting of polymer (PLA) structural components during demonstration.

Sensitive features that need to be re-evaluated or monitored when implementing SMA wire in this design were (1) the fragile connections between the SMA wire to fixtures and (2) the risk of overheating the wire.

Energy Recovery from Waste Heat

The objective of this challenge was to design a cost-effective actuator system using an SMA material to capture thermal energy as the fluid media.

Minimal hardware design constraints are listed in Table 2 and were given for this challenge to be relatively open-ended. Teams had the opportunity to select either air or water thermal fluid sources, where the customer varied in each case. For liquid (water) based thermal fluid sources where the application would be industrial or geothermal processes, the value of power was typically priced at \$1/W with a maximum fluid temperature of 95 °C. Conversely,

for air-based thermal sources (e.g., remote-power or air-craft applications), the value of power was much higher generally but depended on the specific use case. Additionally, the maximum fluid temperature was estimated to be 250 °C, with ambient air or water conditions used to model the cooling media (depending on the operating environment). Generally, the constraints in both cases amounted to providing quantifiable value exceeding the cost of implementation.

Hardware Study III

Team HERO: Heat Energy Recovery On-Demand John Fuller, Ben English, Chris Beebe, and Miller Kettle Project HERO from the Colorado School of Mines demonstrated comprehensive design and multi-physics analysis for a passive linear generator driven by thermally activated NiTi springs. The generator uses electromagnetic induction produced via three neodymium magnets moving through wound copper coils. The system is designed to

Table 2 Energy recovery hardware design requirements presented by CASMART challenge guidelines

Requirements	Description
Thermal fluid source	Air or water
Value of power	Marketable value for thermal fluid source (e.g., water source values \$1/W at max. temperature of 95 °C)
Maximum operating temperature	250 °C
Minimum operating temperature	Room temperature



oscillate using four high carbon steel bias springs and four SMA springs. The final design can be grouped into two main subsystems: (1) the passive inlet valve and (2) the electromagnetic driving piston, both shown in Fig. 4a below. This concept is designed to be mounted underneath an airplane wing by the engine (such as a Boeing 787) and use the waste heat from the engine to actuate and create energy.

The passive inlet valve (Fig. 4a) consists of an oscillating system designed to allow cold air, followed by hot air, into the chamber while only allowing one or the other at a single time. When hot air is flowing into the chamber (shown on the right in Fig. 4c) this heats up the SMA spring, causing it to actuate to the closed position, thus closing off the hot inlet and opening the cold inlet.

The cold air can then enter the system, cooling the SMA spring. The steel bias spring aids in returning the SMA spring to its original position, thus again opening the hot inlet and closing the cold inlet, wherein the cycle repeats. The hot and cold air is also used to heat and cool the actuation system for the electromagnetic driving piston to create energy.

The electromagnetic driving piston system consists of three neodymium magnets passing through a PVC shaft 12.7 cm long wrapped in 5000 turns of 30 gauge insulated copper wire, as shown in Fig. 4b. The system works much the same way as the passive inlet valve. Hot air from the passive inlet valve heats up the four SMA springs attached to the piston which is also attached to the neodymium magnets. The heat causes the SMA springs to close, pulling the magnets through the copper coils generating a current. When cold air enters the system, it causes the SMA springs

to cool, and the four steel bias springs (shown in Fig. 4c) aid in returning the SMA springs to their original position, again pulling the magnets through the copper coils.

The goal of this design was to convert waste heat from jet aircraft to electrical power; however, the low duty cycle capabilities of the material combined with manufacturing challenges resulted in a mostly non-functional prototype. To summarize several of the results from this work:

- Established design metrics from a 2018 SBIR solicitation, with a power density of 50 W/kg and a 50% Carnot efficiency [47].
- Designed an innovative linear generator and conducted thermal, electromagnetic, and structural analysis prior to prototype construction to validate design metrics.
- Early prototype design/application was reliant on high cycle time to produce power, creating challenges given that SMAs are known for their low cycle high-force performance in actuation applications [48].

Tourniquet

The objective was to improve the tourniquet system by incorporating an innate locking mechanism of SMAs when biased against a linear spring.

Teams were challenged to design a tourniquet with a minimum 20-mm-wide contact area for peripheral applications and the length to meet 99th percentile leg size at the maximum circumference. The design had to be capable of being placed and activated with single-handed operation to either an arm or a leg, with placement 25 to 50 mm above the wound site, or directly on the wound site for junction

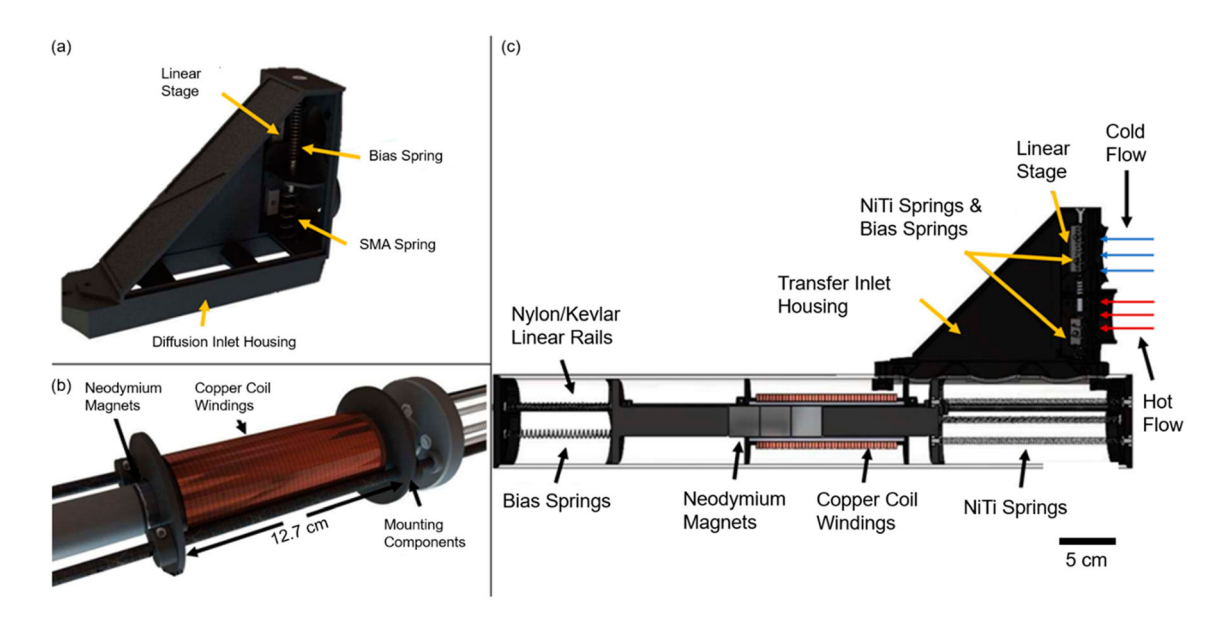


Fig. 4 Linear generator design consisting of a the passive inlet valve actuation system and b the electromagnetic driving piston system. The entire assembled system is shown in c



Table 3 Tourniquet hardware design requirements presented by CASMART challenge guidelines

Requirements	Description	Requirements	Description
Dimension	Minimum 20-mm-wide contact area 99th percentile leg size	Operation	Single hand use to arms or legs
			Self-regulating for correct and constant pressure
Pressure	Circumferential applications: 30 to 60 kPa	Placement	25 to 50 mm above wound site
	Direct applications: 150 N		Directly on wound for junction applications
Activated	Passively or actively with possible manual backup	Actuation time	$\leq 1 \text{ min}$

applications. Pressure was required to be 30 to 60 kPa for circumferential applications and 150 N for direct applications, and self-regulating to ensure correct and constant pressure. Designs could be passively or actively actuated, with the possibility of a manual backup in case of device failure. Overall application and activation time was to be less than 1 min. Tourniquet hardware requirements are summarized in Table 3.

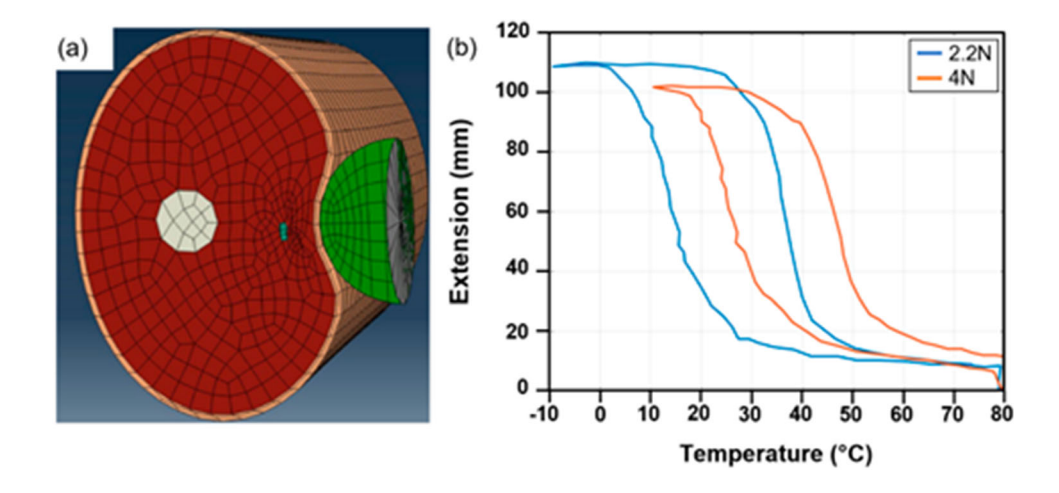
Hardware Study IV

Team TAMU Tourniquet: Brady Allen, Parker Reaume, and Cody Shelton The team from Texas A&M University had the goal of demonstrating the feasibility of designing an innate locking mechanism by incorporating SMAs biased against a linear spring. By characterizing the SMA springs, the ideal spring to bias it against was determined and created by changing the material and geometry of the fabric. This concept allows the tourniquet to lock at a specified force within the hysteresis curve and eliminates the need for extended power application or excessive heat and does not require an external locking mechanism. The tourniquet's design simulation involved creating models of fluid structure interaction of the arm artery system. These models were made in MATLAB and Abaqus and

incorporated blood flow through a stenosed artery and tourniquet arm interaction. The design goal was to target the artery specifically and reduce the total pressure applied to the arm, which minimizes the risk of future tissue damage and the pain experienced. The Abaqus arm model utilized for tourniquet design choices is shown in Fig. 5a). To summarize several of the results from this work:

- Force-displacement testing was done on linear models of the 1/4 in. threaded bolt NiTi #8 and the tightly packed NiTi #8. The data from these tests supported the conclusion that the tightly packed springs are the most efficient for this tourniquet design, as they can apply greater forces and distributing those forces over a small area.
- Tensile characterization results are shown in Fig. 5b on the rod-geometry spring via constant-load thermal cycling at 2.2 N and 4 N. Under 4 N of load, the extension of the spring was likely greater before thermal cycling, resulting in less extension due to transformation.
- The tourniquet contracted maintaining closure and occluding blood flow if the power source supplied the necessary current to heat the wire above A_f.

Fig. 5 a Abaqus model of human arm under compressive loads due to tourniquet shown with **b** iso-force thermal cycles of SMA springs performed at 2.2 and 4 N





Materials Designs

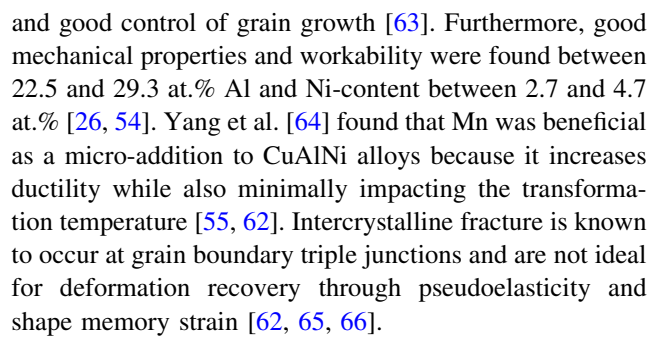
SMAs can be found in various compositions; the three most common SMAs are NiTi-based, Cu-based, and Febased alloys [26, 27]. Binary NiTi alloys are the widely used SMAs currently available; however, their transformation temperatures are limited to about 115 °C, and ternary additions are in development [24]. Cu-based alloys can exhibit high transformation temperatures but suffer from low fatigue life due to microstructural challenges [49]. Fe-based SMAs have sufficiently high transformation temperatures and exhibit magnetic characteristics, adding an unnecessary property to the presented case studies.

Niti-Based Alloys

NiTi-based alloys have led the way since the early 1960s in technological innovations for SMA materials as active, adaptive smart systems. The U.S. Naval Ordnance Laboratory developed and commercialized NiTi alloys in the 1960s under the trademark Nitinol. The medical field commonly utilizes the pseudoelastic effect when designing SMAs for medical stents, eyeglasses, and orthodontia, as NiTi is known to be biocompatible [50–52]. The microstructure associated with phase transformation in NiTi-based alloys typically involves two phases: a highly symmetrical cubic B2 structure austenite phase and a lowsymmetry monoclinic B19' structure martensite phase. Martensite exhibits other crystal structures such as a rhombohedral or orthorhombic structure from processing, compositional changes such as ternary additions, or a combination of the two. The addition of ternary elements such as Hf, Zr, Pd, and Pt is of high interest in aerospace applications for their ability to increase transformation temperatures and facilitate thermal hysteresis attunement. Most industries cannot justify the cost to commercialize ternary alloys with Au, Pd, or Pt, consequently limiting uses to niche applications.

CuAl-Based Alloys

Polycrystalline Cu-based high-temperature SMAs are chosen for some projects because they have significantly lower densities than their NiTi-based and Fe-based counterparts [53–55] and exhibit a higher elastic modulus [56, 57]. Generally, the NiTi martensite elastic modulus has been reported in the range of 20 to 70 GPa and CuAl alloys range from 60 to 170 GPa [58–61]. The primary challenges with polycrystalline binary CuAl are poor cold workability and poor martensitic stability [55, 62]. Ternary CuAlNi alloys with less than 27.1 at.% Al were found to have a smooth hysteresis with high thermoelastic behavior



Two major approaches to increasing ductility in Cubased SMAs are: (1) grain refinement [67-70] and (2) utilization of single-crystal materials [64, 66, 71]. In some cases, single crystal Cu-based SMAs have demonstrated extraordinary pseudoelasticity strain upwards of 40% [72]. However, the production expense of single-crystal and the brittleness of polycrystalline SMAs hinder the usefulness of these materials. A potential solution was found in a novel microstructure termed "oligocrystalline." Bamboostructured SMAs are a subset of oligocrystalline materials in which the grains are layered lengthwise (like bamboo) and the cross-sectional grain size is equivalent to the cross section of the wire [66]. This bamboo structure produces pseudoelastic strains up to 4 times larger than bulk polycrystalline and is effective at suppressing intergranular fracture, common in bulk polycrystalline materials. This is due in part to a lack of triple junctions, a high specific area, and small-diameter grains [65, 66, 73].

Deployment and Orientation Mechanism for Smallsats

The objective of the project was to design an SMA that conforms to the design constraints for application in a 3U CubeSat as an actuation device.

The materials design teams were challenged with several functional requirements and processing constraints that the material chosen (i.e., SMA) should meet to be viable in passive actuation systems. Constraints are summarized in Table 4 and were prioritized as primary or secondary to simplify the selection process. Primary constraints included (1) austenite finish temperature range at 120 ± 10 °C, and (2) alloying elements (no use of precious metals, Hf, or Zr). Secondary constraints included (1) recoverable actuation strains greater than 3.5% and (2) processability by conventional means, defined by the team as hot rolling and cold drawing.

Materials Study I

Team Metallurgica: Faith Gantz, Mora Issa, Skye Segovia, and Xiaowei Wang The team from the University of North Texas prioritized the material design using



Requirements	Description	Requirements	Description
Transformation temperature	$A_{\rm f}$ = 120 \pm 10 °C at zero external stress	Cost	No precious metals (e.g., Au, Pt, Pd) or Hf, Zr
Actuation strain	3.5% recoverable strain	Property attunement methods	Control properties through processing methods
Slope $(A_f - A_s)$	Minimize variance and define method	Production method	Conventional methods
Actuation cycle	> 20 cycles	Melt purity	C < 0.03 wt%, O < 0.08 wt%
Actuation time	< 30 s	Form	Processable into useable form (e.g., wire, rod, and plate)

Table 4 3U CubeSat materials design requirements presented by CASMART challenge guidelines

fundamental concepts to choosing a composition suitable for processing using conventional methods (e.g., rolling) into wire. Potential alloying elements were selected and compiled in a Darken-Gurry map, which uses Pauling rules to determine the solubility of selected elements with a less than 7% (inner ring) and 15% (outer ring) difference as compared with Cu (Fig. 6). Based on a literature review [54, 63, 64], alloying additions of Ni, Mn, and Al to the Cu-based SMA were chosen to pursue the formation of a bamboo structure and to fulfill the design requirements [63]. A linear interpolation sensitivity analysis was used to determine the specific compositions [27, 54, 74]. CuAlNiMn alloys were homogenized at 850 °C for 1 h and quenched in H₂O to achieve a martensitic structure. Samples were preheated at 700 °C for 30 min and hot rolled into plates at 25, 50, and 75% reduction with 5 min intermediate annealing between passes, respectively. The plates were cut into strips in preparation to hot rolling the wire using wire rolling die and the same anneal-roll procedures as the plates. For an initial observation of the effect of grain growth in the material, wires were heat-treated at 850 and 950 °C in air for 30 and 90 min each [54].

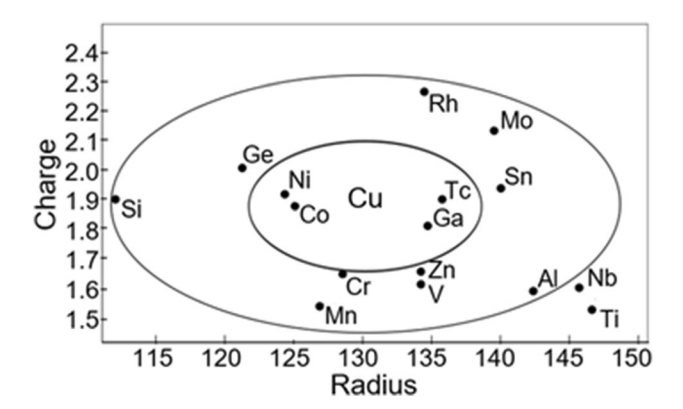


Fig. 6 Darken-Gurry solubility map of copper

To summarize several of the key results and takeaways from this work:

- Cu_{70.3}Al_{26.3}Ni_{2.7}Mn_{0.7} at.% with A_f of 124 °C in the homogenized state met the project transformation temperatures requirement. The transformation temperatures increased to 159 °C in the 25% reduction condition and 139 °C in the 50% reduction, all while maintaining a sharp enthalpy peak.
- Wire of 1 mm diameter (75 to 89% thickness reduction) was achieved using the rolling parameters of 700 °C with a 30-min preheat and 5-min intermediate heating between passes.
- Hot rolling the material promotes preferred grain orientation beneficial to sequential heat treatments; however, work hardening leads to an increase in dislocation density/plasticity, which counteracts subsequent grain growth. Further investigation with a finer diameter wire is required to determine the optimal heat treatments to promote rapid grain growth.

Energy Recovery from Waste Heat

The objective was to design an SMA material for an actuator system that captures and releases thermal energy to optimize mechanical power.

Wastewater is a much denser media than gas, allowing for much faster heat transfer. The most important characteristics for the design were the alterations of transformation temperatures and hysteresis size and the impact of each addition on these temperatures: a small hysteresis (< 25 °C) along with temperature transformation of $A_{\rm f}$ = 90 °C and $M_{\rm f}$ = 25 °C due to the wastewater and ambient air temperature, respectively. Maximum stress had to support a large work output and maintain a stable value of actuation strain for extended periods of time to ensure the domestic conversion application was priced at \$1/W.



Table 5 Energy recovery material design requirements presented by CASMART challenge guidelines

Requirements	Description	Requirements	Description (°C)
Thermal fluid source	Water	Hysteresis	< 25
Value of power	\$1/W at max. temperature of 95 °C	$A_{ m f}$	90
		$M_{ m f}$	25

Design requirements for the energy recovery material challenge is summarized in Table 5.

Materials Study II

Team Power Rangers: Sharon Pearlnath, Bianca Avila, John Broucek, and Ben Rudzinski Research from Texas A&M University team details the analysis of four different element additions to NiTiCu-based SMA systems [75]. The goal of maximizing work output while maintaining the fatigue life of samples was considered a priority. Ni_{43.5}- $Ti_{50}Cu_5Co_{1.5}$, $Ni_{44}Ti_{49}Cu_6Hf_1$, $Ni_{42.3}Ti_{29.7}Cu_5Hf_{20}Fe_3$, and Ni₄₄Ti_{46.5}Cu_{6.5}Zr₃ were melted with vacuum arc melting with near-100% pure elements cut with electrical discharge machining (EDM), quartz encapsulated under argon, treated with a solution heat treatment (SHT) of 950 °C for 12 h, quenched, hot-rolled (by 20% reduction in thickness) at 850 °C, and age-treated at either 350 or 550 °C for 12 h. Transformation temperatures were tested with DSC. Based on the results, Ni_{43.5}Ti₅₀Cu₅Co_{1.5} was further tested with isobaric loading ranging between 0 and 500 MPa. The transformation temperature results and the loading path under 150 MPa can be found in Table 6 and Fig. 7, respectively.

To summarize several of the key results and takeaways from this work:

• The material Ni_{43.5}Ti₅₀Cu₅Co_{1.5} A_f was within 10 °C and the ΔT was within 6 °C of the material requirement while thermally cycling under 150 MPa of stress. An acceptable 4% actuation strain recovered during the thermal cycle, as featured in Fig. 7. No cracking was observed in the sample under any tested stresses; however, irrecoverable strain increased considerably with stress levels 300 to 500 MPa (ε_{irr} = 1.7 to 4.5%).

Table 6 Transformation temperatures of $Ni_{43.5}Ti_{50}Cu_5Co_{1.5}$ after solution treatment 950 °C for 12 h and hot-rolled at 850 °C under 150 MPa load

Transformation temperatures (°C)	
$M_{ m f}$	65
M_{s}	68
A_{s}	90
$A_{ m f}$	99
$\Delta T_{\rm H} = (A_{\rm f} - M_{\rm s})$	31

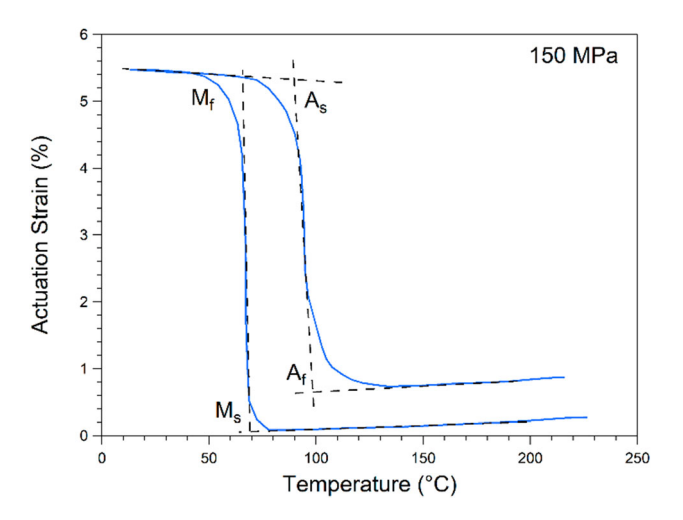


Fig. 7 Temperature vs. strain plot of $Ni_{43.5}Ti_{50}Cu_5Co_{1.5}$ under 150 MPa tension load

- The calculated work output using stress of 150 MPa and actuation strain of 3.69% produces a final work output result of 0.927 J/g. This value is incredibly high, especially when compared with the benchmarks for work output established in other literature [19, 76, 77].
- Ni_{42.3}Ti_{29.7}Cu₅Hf₂₀Fe₃ was found to be challenging to process, and SHT suppressed the martensitic transformation of the material. Ni₄₄Ti₄₉Cu₆Hf₁ performance was dominated by precipitate generation, leading to an undesirable widened hysteresis and reduced ductility.
- Ni₄₄Ti_{46.5}Cu_{6.5}Zr₃ similarly experienced precipitate formation. While aging treatments reduced the size of the precipitates and improved ductility, such treatments increased transformation temperatures above the desired level.

Spinal Curvature Correction Device

The objective was to design an externally worn pseudoelastic brace that works similarly to orthodontic hardware but maintains tension longer.

Desired transformation temperatures for the alloy used in the correction device were $M_{\rm f}$ slightly above 0 °C and $A_{\rm f}$ between 20 and 30 °C. This would allow a constant wearable stress throughout a range of strains because of the material's pseudoelasticity. The temperatures of these materials could be reduced using an ice pack to drive the alloy into the martensitic phase and reduce the amount of



 Table 7
 Spinal curvature correction materials design requirements

 presented by CASMART challenge guidelines

Requirement	Description
Temperatures	M_f slightly < 0 °C
	$A_f = 20 ^{\circ}\text{C}$ to 30 $^{\circ}\text{C}$
Austenite plateau stress	138 MPa/20 ksi
Applied pressure	110.3 kPa/16 psi
Cycles	912

stress required to unload the brace, leading to easier removal. The alloy design had to consider beneficial properties such as corrosion resistance, biocompatibility, and light weight. The desired stresses for the alloy's austenite plateau were 20 to 30 ksi to maintain enough force for the spine correction without causing the patient discomfort or injury [78]. Ideally a patient would remove the brace once a day, with a maximum wearable life of 2.5 years, which equates to a maximum of 912 cycles. Design requirements for the Spinal curvature correction material challenge is summarized in Table 7.

Materials Study III

Team Immaculé: Myly Fabre, Brandon King, Matthew LeBeau, and Sydney Nelson The team from Colorado School of Mines began by determining the optimal transformation temperatures for this application to enable full transformation at body temperature ($A_{\rm f} = 20$ to 30 °C, $M_{\rm f} = 0$ °C) with 20 to 30 ksi. The stress would be controlled through stress-induced martensitic transformation or with an ice pack by temperature-induced transformation to

avoid discomfort for the user. Other material characteristics, such as biocompatibility, weight, cost, and fatigue life, were considered in the selection of the two alloy systems. The alloy systems NiTiHf and CuAlNi were chosen to develop for the application. The team constructed a heat treatment matrix to evaluate several conditions, using heat treatment procedures from recent literature to tailor transformation temperatures of Ni-rich NiTiHf alloy systems utilizing H-phase precipitation [79]. For CuAlNi, standard and cyclic heat treatments were evaluated based on grain growth effects to minimize the stress hysteresis. Pseudoelasticity and stress to failure were tested under the following conditions: the Ni₅₁Ti_{36.5}Hf_{12.5} alloy was solution treated at 1050 °C for 24 h and aged in air at 550 °C for $3.5\ h$ and air cooled, and the $Cu_{68.74}Al_{27.15}Ni_{4.11}$ was annealed at 900 °C for 20 min, furnace cooled at a rate of 3.3 °C/min to 500 °C for 10 min followed by a 10 °C/min temperature increase to 900 °C for 60 min, then water quenched. Both alloy systems demonstrated pseudoelasticity at 25 °C as shown in Fig. 8a and b, respectively. The stress to failure results for Ni₅₁Ti_{36.5}Hf_{12.5} alloy to exhibit compression strength to be nearly 1900 MPa while the Cu_{68.74}Al_{27.15}Ni_{4.11} alloy exhibited 620 MPa. The Clausius-Clapeyron relation was used to determine the loading stress at body temperature 37 °C.

To summarize several of the key results and takeaways from this work:

• Ni₅₁Ti_{36.5}Hf_{12.5} showed no transformation via DSC within the range of -150 °C to 150 °C; however, the alloy demonstrated pseudoelasticity behavior with a martensitic starting stress (σ_s^M) = 26.99 MPa and a stress hysteresis of 6.82 MPa. The loading stress at 37 °C was predicted to be 97.2 MPa using the Clausius–Clapeyron relation.

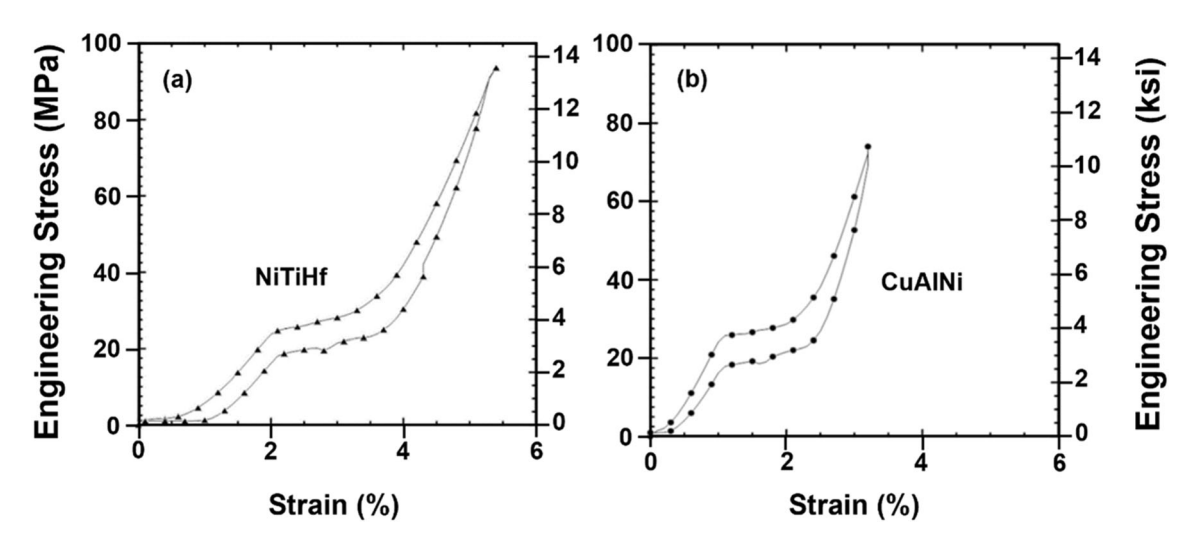


Fig. 8 a Compression test response for NiTiHf at 25 °C showing pseudoelastic response after heat treatment. b Compression test response for CuAlNi at 25 °C showing pseudoelastic response after heat treatment



- $\text{Cu}_{68.74}\text{Al}_{27.15}\text{Ni}_{4.11}$, which exhibited transformation temperatures closest to body temperature, was validated via compression testing with a $\sigma_s^M = 26.68$ MPa and hysteresis = 7.62 MPa. The loading stress at 37 °C was predicted to be 62.68 MPa using the Clausius–Clapeyron relation. Microscopy images of the CuAlNi alloy systems showed columnar grains in the range of 800 to 900 nm. A stress relief heat treatment is recommended to be performed in further development due to brittle alloys breaking prematurely. It is also recommended that different geometries be evaluated to determine the effects of grain structure on performance.
- Overall, each material met the desired design requirements and should help in the development of new scoliosis braces. The NiTiHf alloy would be a better option for higher strength, but the CuAlNi alloy would be a cost-effective alternative.

Conclusion

This paper presented research from a biennial student design competition hosted by Consortium for the Advancement of Shape Memory Alloy Research and Technology (CASMART) in which teams address realworld problems facing the shape memory alloy (SMA) community and receive guidance and feedback from CASMART members. The CASMART Student Design Challenge is meant to inspire the next generation of SMA research and is used as an outreach strategy to promote the implementation of state-of-the-art designs with SMA technology. Results from 7 of the 14 teams competing in the CASMART 3rd Student Design Challenge were presented in this paper. Each of the case studies presented adopted one of two design perspectives: to design the material or to design with the material. The general outcomes of the CASMART 3rd Student Design Challenge may be summarized as follows:

- More complex designs presented more challenges. Several cases began with interesting but complex designs. Complex design can refer to the number of mechanical components and geometries, or for materials, examining a combination of compositions, processing methods, and thermo-mechanical response. As an initial assessment, it is recommended to start with designing the degree of freedom to isolate the complexity.
- Time and budget constraints limited redesign and refabrication of the necessary components to support a new linear motion system, so results were evaluated on a component level by testing subsystems

- individually and comparing results to initial analysis. Timeframe and budgetary restrictions on the project limited the number of parts that could be redesigned, and further thermal analysis and material selection to accommodate expected temperatures will need to be incorporated in future work.
- Designing with SMAs can be circular (material properties can vary widely across alloy systems and manufacturing and are hard to choose to meet a design specifications/requirements.
- Characterizing high-cycle fatigue, load-bias testing should be performed utilizing the same heat treatment cycles, in which SMA samples are loaded to the predicted electromagnetic reactive loading conditions expected in the device's operation and then thermally cycled using a programmable power supply and a joule heating circuit or similar mechanism for cycling.
- Alloy composition design and processing parameters require a systematic approach to isolate effects caused by solutionizing, aging, and other processing methods. Experimental variables such as elemental additions, time, and temperature will affect a variety of material characteristics, such as the type, the size, and the distribution of precipitate or the ductility while being mechanically worked.

Acknowledgements Special recognition goes to the winning teams: Hardware design: Sat³UNT, "Novel Application of Shape Memory Alloys for CubeSat Solar Array Actuation." Team members included Kelsa Adams, Michael Ayers, Jordan Barnes, Robert Boone, David Evers, and Brittany Thurstin. Mentored by Robert W. Wheeler, Richard Z. Zhang, and Marcus L. Young. Material design: Immaculé, "Design, fabricate, and validate a shape memory alloy suitable for integration into a next-generation brace for scoliosis patients." Team members included Myly Fabre, Brandon King, Matthew LeBeau, and Sydney Nelson. Mentored by Aaron P. Stebner and Othmane Benafan. All student authors give special thanks to Dr. Othmane Benafan (NASA) and Consortium for the Advancement of Shape Memory Alloy Research and Technology (CASMART) for providing the opportunity, acting as valuable guides, and offering time and facilities to process and characterize material as necessary. NSF Award 1926074 financially supported student participation in the design competition by funding travel costs to attend the conference. The authors would also like to acknowledge NASA for providing materials; Drew Forbes (Fort Wayne Metals) for providing SMA actuator wire and material information; Classic Steel LLC for providing steel channel and machining capabilities; Confluence Medical for providing their test facilities; Nathan A. Ley (UNT) for advice on composition and processing; Dr. Richard Z. Zhang (UNT) for advice on design construction; Dr. Kristi Shyrock, Doug Nicholson (The Boeing Company), and Peter Jardine (Shape Change Technologies) for guidance through the initial design requirement derivation process; Garrison Hommer, Tejas Umale, Woohyum Cho, Michayal Mathew, and all graduate, undergraduate, and postdoctoral students and staff involved in the projects at each respective university (you know who you are). The authors would like to thank UNT's Materials Research Facility (MRF) for access to facilities and equipment. The synchrotron radiation x-ray diffraction research used resources of the Advanced Photon Source, a U.S. Department of Energy (DOE) Office



of Science User Facility operated for the DOE Office of Science by Argonne National Laboratory under Contract No. DE-AC02-06CH11357. A special thank you to all the sponsors who supported the students' travel including Euroflex, Dynalloy, Inc, Fort Wayne Metals, Gore, Admedes, NASA, NSF and Mr. Brian Van Doren. A special thank you to SMST and ASM International for sponsoring the conference fees, Nitinol workshop and other student events.

References

- Buehler W, Gilfrich J, Riley R (1963) Effect of low-temperature phase changes on the mechanical properties of alloys near composition Ti–Ni. Appl Phys 34:1475–1477
- Jani JM, Leary M, Subic A, Gibson MA (2014) A review of shape memory alloy research, applications and opportunities. Mater Des 1980–2015(56):1078–1113
- 3. Jani JM, Leary M, Subic A (2014) Shape memory alloys in automotive applications. Appl Mech Mater 663:248–253
- Chaudhari R, Vora JJ, Parikh DM (2021) A review on applications of nitinol shape memory alloy. In: Recent Advances in Mechanical Infrastructure. Springer, pp 123–132
- Cross WB, Kariotis AH, Stimler FJ (1969) Nitinol characterization study. NASA, Langley Research Center
- Jackson CM, Wagner HM, Wasilewski RJ (1972) 55-Nitinol-the alloy with a memory: it's physical metallurgy properties, and applications. NASA SP-5110, vol 5110. NASA Special Publication
- 7. Duerig TW, Melton KN, Stöckel D (2013) Engineering aspects of shape memory alloys. Butterworth-Heinemann, Oxford
- Calkins FT, Mabe JH (2010) Shape memory alloy based morphing aerostructures
- Derby S, Sreekumar M, Nagarajan T, Singaperumal M, Zoppi M, Molfino R (2007) Critical review of current trends in shape memory alloy actuators for intelligent robots. Ind Robot
- Rodrigue H, Wang W, Han M-W, Kim TJY, Ahn S-H (2017) An overview of shape memory alloy-coupled actuators and robots. Soft Robot 4(1):3–15
- Sutou Y, Omori T, Wang JJ, Kainuma R, Ishida K (2004) Characteristics of Cu–Al–Mn-based shape memory alloys and their applications. Mater Sci Eng A 378(1–2):278–282
- Schmidt M, Schütze A, Seelecke S (2015) Scientific test setup for investigation of shape memory alloy based elastocaloric cooling processes. Int J Refrig 54:88–97
- Hou H et al (2019) Fatigue-resistant high-performance elastocaloric materials made by additive manufacturing. Science 366(6469):1116–1121
- Zareie S, Issa AS, Seethaler RJ, Zabihollah A (2020) Recent advances in the applications of shape memory alloys in civil infrastructures: a review. Structures 27:1535–1550. https://doi. org/10.1016/j.istruc.2020.05.058
- Costanza G, Tata ME (2020) Shape memory alloys for aerospace, recent developments, and new applications: a short review. Materials 13(8):1856. https://doi.org/10.3390/ma13081856
- Lockney D. Mechanical and Fluid Systems Superelastic Tire. National Aeronautics and Space Administration. https://technology.nasa.gov/patent/LEW-TOPS-99
- Benafan O, Moholt MR, Bass M, Mabe JH, Nicholson DE, Calkins FT (2019) Recent advancements in rotary shape memory alloy actuators for aeronautics. Shape Mem Superelast 5(4):415–428
- Wheeler III RW (2017) Actuation fatigue characterization methods and lifetime predictions of shape memory alloy actuators. https://hdl.handle.net/1969.1/161597

- Casalena L et al (2017) Mechanical behavior and microstructural analysis of NiTi-40Au shape memory alloys exhibiting work output above 400 °C. Intermetallics 86:33–44. https://doi.org/10. 1016/j.intermet.2017.03.005
- Demblon A et al (2022) Compositional and microstructural sensitivity of the actuation fatigue response in NiTiHf high temperature shape memory alloys. Mater Sci Eng A 838:142786. https://doi.org/10.1016/j.msea.2022.142786
- Young ML et al (2019) Characterization and processing of high temperature shape memory alloys for aerospace applications. In: AIAA Scitech 2019 Forum, p 1196
- Kota S, Hetrick J, Li Z, Saggere L (1999) Tailoring unconventional actuators using compliant transmissions: design methods and applications. IEEE/ASME Trans Mechatron 4(4):396–408. https://doi.org/10.1109/3516.809518
- Hartl DJ, Lagoudas DC, Calkins FT (2011) Advanced methods for the analysis, design, and optimization of SMA-based aerostructures. Smart Mater Struct 20(9):94006. https://doi.org/ 10.1088/0964-1726/20/9/094006
- Benafan O et al (2014) Shape memory alloy actuator design: CASMART collaborative best practices and case studies. Int J Mech Mater Des 10(1):1–42
- Caltagirone PE et al (2021) Shape memory alloy-enabled expandable space habitat—case studies for second CASMART student design challenge. Shape Memory Superelast 1–24
- Lagoudas DC (2008) Shape memory alloys: modeling and engineering applications. Springer, New York. https://doi.org/10. 1007/978-0-387-47685-8
- 27. Ma J, Karaman I, Noebe RD (2010) High temperature shape memory alloys. Int Mater Rev 55(5):257–315
- Wheeler III RW (2017) Actuation fatigue characterization methods and lifetime predictions of shape memory alloy actuators. Texas A & M University
- Puig-Suari J, Turner C, Ahlgren W (2001) Development of the standard CubeSat deployer and a CubeSat class PicoSatellite. In: 2001 IEEE Aerospace Conference Proceedings (Cat. No. 01TH8542), vol 1, pp 1–347
- Woellert K, Ehrenfreund P, Ricco AJ, Hertzfeld H (2011) Cubesats: Cost-effective science and technology platforms for emerging and developing nations. Adv Space Res 47(4):663–684
- Swartwout M (2011) Attack of the CubeSats: A Statistical Look (SSC11-VI-04). In: 25th Annual AIAA/USU Conference on Small Satellites
- 32. Hunter R, Korsmeyer D (2015) A Review of NASA Ames CubeSat Program
- Subbian J, Raikwar S, Sindam NK, Madhav MT, Anand PI (2021) Design and development of NiTi shape memory alloy belt for waste heat energy recovery system. J Mater Eng Perform 30(12):9048–9058. https://doi.org/10.1007/s11665-021-06091-7
- 34. Qian S et al (2016) A review of elastocaloric cooling: materials, cycles and system integrations. Int J Refrig 64:1–19. https://doi.org/10.1016/j.ijrefrig.2015.12.001
- Qian S, Wang Y, Yuan L, Yu J (2019) A heat driven elastocaloric cooling system. Energy 182:881–899. https://doi.org/10.1016/j. energy.2019.06.094
- Kumar PK, Lagoudas DC (2008) Introduction to shape memory alloys. shape memory alloys modeling and engineering applications. Springer, New York
- Consortium for the Advancement of Shape Memory Alloy Research and Technology. CASMART SMA Actuator Design Tool (2018)
- Fayssoux RS, Cho RH, Herman MJ (2010) A history of bracing for idiopathic scoliosis in North America. Clin Orthopaedics Relat Res 468(3):654–664



- 39. Chan W-Y et al (2018) Mechanical and clinical evaluation of a shape memory alloy and conventional struts in a flexible scoliotic brace. Ann Biomed Eng 46(8):1194–1205
- Ali A, Fontanari V, Fontana M, Schmölz W (2021) Spinal deformities and advancement in corrective orthoses. Bioengineering 8(1):2
- Nachemson AL et al (1995) Effectiveness of treatment with a brace in girls who have adolescent idiopathic scoliosis. A prospective, controlled study based on data from the Brace Study of the Scoliosis Research Society. J Bone Joint Surg Ser A 77(6):815–822
- 42. Wong MS et al (2008) The effect of rigid versus flexible spinal orthosis on the clinical efficacy and acceptance of the patients with adolescent idiopathic scoliosis. Spine 33(12):1360–1365
- Coillard C, Leroux MA, Zabjek KF, Rivard C (2003) SpineCor–a non-rigid brace for the treatment of idiopathic scoliosis: posttreatment results. Eur Spine J 12(2):141–148
- 44. Safranski D, Dupont K, Gall K (2020) Pseudoelastic NiTiNOL in orthopaedic applications. Shape Mem Superelast 6(3):332–341
- GSFC (2021) GSFC-STD-7000 REV B General Environmental Verification Standard (GEVS) for GSFC Flight Programs and Projects. Greenbelt
- 46. National Aeronautics and Space Administration (2022) DESIGN AND DEVELOPMENT REQUIREMENTS FOR MECHAN-ISMS. NASA-STD-5017, 2016. https://standards.nasa.gov/stan dard/nasa/nasa-std-5017. Accessed: March 21
- DoD 2018.3 SBIR Solicitation (2018) Shape memory alloy heat engine
- 48. Moholt M, Benafan O (2017) Spanwise adaptive wing. In: 3rd annual convergent aeronautics solutions showcase and innovation faire, pp 19–20
- Husain SW, Clapp PC (1988) The effect of aging on the fracture behavior of Cu-AI-Ni jo phase alloys. Metall Trans A 19(7):1761–1766
- Stoeckel D, Pelton A, Duerig T (2004) Self-expanding nitinol stents: material and design considerations. Eur Radiol 14(2):292–301
- Hurst CL, Duncanson MG Jr, Nanda RS, Angolkar PV (1990) An evaluation of the shape-memory phenomenon of nickel-titanium orthodontic wires. Am J Orthod Dentofac Orthop 98(1):72–76
- Hodgson DE, Zider RB (1988) Shape-memory alloy resetting method. Google Patents
- 53. Guerioune M et al (2008) SHS of shape memory CuZnAl alloys. Int J Self Propag High Temp Synth 17(1):41–48
- Dasgupta R (2014) A look into Cu-based shape memory alloys: present scenario and future prospects. J Mater Res 29(16):1681–1698
- Alaneme KK, Okotete EA (2016) Reconciling viability and costeffective shape memory alloy options—a review of copper and iron based shape memory metallic systems. Eng Sci Technol Int J 19(3):1582–1592
- Čolić M et al (2010) Relationship between microstructure, cytotoxicity and corrosion properties of a Cu–Al–Ni shape memory alloy. Acta Biomater 6(1):308–317
- 57. Ivanić I, Gojić M, Kožuh S (2014) Alloys with shape recollection (Part II): the most significant properties. Chem Ind 63(9–10):331–344
- 58. Young ML, Wagner M-X, Frenzel J, Schmahl WW, Eggeler G (2010) Phase volume fractions and strain measurements in an ultrafine-grained NiTi shape-memory alloy during tensile loading. Acta Mater 58(7):2344–2354
- Zhen W, Liu X, Xie J (2011) Effects of solidification parameters on microstructure and mechanical properties of continuous columnar-grained Cu–Al–Ni alloy. Prog Nat Sci 21(5):368–374

- Morris MA, Lipe T (1994) Microstructural influence of Mn additions on thermoelastic and pseudoelastic properties of Cu Al Ni allovs. Acta Metall Mater 42(5):1583–1594
- Yang J et al (2022) First-principles study of the effect of aluminum content on the elastic properties of Cu-Al alloys. Mater Today Commun 31:103399. https://doi.org/10.1016/j.mtcomm. 2022.103399
- Tadaki T, Otsuka K, Shimizu K (1988) Shape memory alloys.
 Annu Rev Mater Sci 18(1):25–45
- 63. Saud SN, Hamzah E, Abubakar T, Bakhsheshi-Rad HR, Zamri M, Tanemura M (2014) Effects of Mn additions on the structure, mechanical properties, and corrosion behavior of Cu-Al-Ni shape memory alloys. J Mater Eng Perform 23(10):3620–3629
- 64. Yang Q et al (2018) Suppressing heating rate-dependent martensitic stabilization in ductile Cu-Al-Mn shape memory alloys by Ni addition: an experimental and first-principles study. Mater Charact 145:381–388
- Ueland SM, Schuh CA (2013) Grain boundary and triple junction constraints during martensitic transformation in shape memory alloys. J Appl Phys 114(5):53503
- Chen Y, Zhang X, Dunand DC, Schuh CA (2009) Shape memory and superelasticity in polycrystalline Cu–Al–Ni microwires. Appl Phys Lett 95(17):171906
- 67. Van Humbeeck J, Chandrasekaran M, Delaey L (1989) The influence of post quench aging in the beta-phase on the transformation characteristics and the physical and mechanical properties of martensite in a Cu–Al–Ni shape memory alloy. ISIJ Int 29(5):388–394
- 68. Gao Y, Zhu M, Lai JKL (1998) Microstructure characterization and effect of thermal cycling and ageing on vanadium-doped Cu– Al–Ni–Mn high-temperature shape memory alloy. J Mater Sci 33(14):3579–3584
- Font J, Muntasell J, Pons J, Cesari E (1997) Thermal cycling effects in high temperature Cu–Al–Ni–Mn–B shape memory alloys. J Mater Res 12(9):2288–2297
- Adachi K, Shoji K, Hamada Y (1989) Formation of X phases and origin of grain refinement effect in Cu–Al–Ni shape memory alloys added with titanium. ISIJ Int 29(5):378–387
- Otsuka K, Wayman CM, Nakai K, Sakamoto H, Shimizu K (1976) Superelasticity effects and stress-induced martensitic transformations in Cu Al Ni alloys. Acta Metall 24(3):207–226
- Oliveira JP et al (2018) Laser welding of Cu-Al-Be shape memory alloys: microstructure and mechanical properties. Mater Des 148:145–152. https://doi.org/10.1016/j.matdes.2018.03.066
- Mazzer EM, da Silva MR, Gargarella P (2022) Revisiting Cubased shape memory alloys: recent developments and new perspectives. J Mater Res 37(1):162–182. https://doi.org/10.1557/ s43578-021-00444-7
- Recarte V, Pérez-Sáez RB, Bocanegra EH, Nó ML, San Juan J (1999) "Dependence of the martensitic transformation characteristics on concentration in Cu–Al–Ni shape memory alloys. Mater Sci Eng A 273:380–384
- 75. Frenzel J, Wieczorek A, Opahle I, Maaß B, Drautz R, Eggeler G (2015) On the effect of alloy composition on martensite start temperatures and latent heats in Ni-Ti-based shape memory alloys. Acta Mater 90:213–231. https://doi.org/10.1016/j.actamat. 2015.02.029
- Atli KC, Karaman I, Noebe RD (2011) Work output of the twoway shape memory effect in Ti50.5Ni 24.5Pd25 high-temperature shape memory alloy. Scripta Mater 65(10):903–906. https://doi. org/10.1016/j.scriptamat.2011.08.006
- Atli KC, Karaman I, Noebe RD, Bigelow G, Gaydosh D (2015) Work production using the two-way shape memory effect in NiTi and a Ni-rich NiTiHf high-temperature shape memory alloy. Smart Mater Struct 24(12):125023. https://doi.org/10.1088/0964-1726/24/12/125023



- Mosekilde L, Mosekilde L, Danielsen CC (1987) Biomechanical competence of vertebral trabecular bone in relation to ash density and age in normal individuals. Bone 8(2):79–85
- 79. Amin-Ahmadi B, Gallmeyer T, Pauza JG, Duerig TW, Noebe RD, Stebner AP (2018) Effect of a pre-aging treatment on the mechanical behaviors of Ni50.3Ti49.7 xHfx (x \leq 9 at.%)

Shape memory alloys. Scripta Mater 147:11–15. https://doi.org/10.1016/j.scriptamat.2017.12.024

Publisher's Note Springer Nature remains neutral with regard to jurisdictional claims in published maps and institutional affiliations.

